1-1-2020

A Hybrid Electrochemical Energy Storage Device Using Sustainable Electrode Materials

Manickam Minakshi

David R. G Mitchell
University of Wollongong, dmitchel@uow.edu.au

Robert Jones

Nimai Pramanik

Annelise Jean-Fulcrand

See next page for additional authors

A Hybrid Electrochemical Energy Storage Device Using Sustainable Electrode Materials

Abstract

2020 Wiley-VCH Verlag GmbH & Co. KGaA, Weinheim A new electrochemical energy storage device, comprising a faradaic rechargeable pseudo-capacitor type electrode with a non-faradaic rechargeable capacitor electrode, is successfully developed for potential applications in smart electric grids. Mapping new electrodes possessing both high energy and power densities as well as long cycle life is vital for the sustainable energy management. In this work, we present a new approach to design electrodes, fabricated from sustainable resources by hybridizing calcined eggshell capacitor anode with a mixed binary metal oxide pseudo-capacitor cathode. Calcium carbonate (calcite), obtained from the biowaste-derived eggshell, is an effective electrode material and operates via accumulation of ions on the electrode surface, providing a high discharge capacitance of 100 F/g through a non-faradaic process. The calcite present in eggshells is found to be a valuable renewable resource which can be utilized for energy storage through suitable process design. Otherwise, such potentially useful materials (eggshells) are generally discarded as landfill. The mixed binary metallic oxide (NiO/Co3O4) showed a typical pseudocapacitive behaviour associated with both charge transfer reactions and electrostatic means provided a high discharge capacitance of 225 F/g. The fabricated prototype hybrid device provides an energy density 35 Wh/Kg at a power density 420 W/Kg. The charge storage characteristics of the hybrid device depend heavily on the current rate employed. The design and fabrication of new sustainable electrode materials provides an understanding of materials and their electrochemical performance in the high-voltage window.

Disciplines

Engineering | Physical Sciences and Mathematics

Publication Details

Minakshi, M., Mitchell, D., Jones, R., Pramanik, N., Jean-Fulcrand, A. & Garnweitner, G. (2020). A Hybrid Electrochemical Energy Storage Device Using Sustainable Electrode Materials. ChemistrySelect, 5 (4), 1597-1606.

Authors

Manickam Minakshi, David R. G Mitchell, Robert Jones, Nimai Pramanik, Annelise Jean-Fulcrand, and Georg Garnweitner

A new hybrid electrochemical energy storage device using sustainable electrode materials

[1]Manickam Minakshi *, [2]David R.G. Mitchell, [3]Robert T. Jones, [4]Nimai Chand Pramanik, [5]Annelise Jean-Fulcrand, and [5]Georg Garnweitner

*[1]Engineering and Energy, Murdoch University, WA 6150, **Australia***
*[2]Electron Microscopy Centre, University of Wollongong, NSW 2500, **Australia***
*[3]Centre for Materials and Surface Science, La Trobe University, VIC 3086, **Australia***
*[4]Aerogel & Energy Material Lab, Center for Materials for Electronics Technology (C-MET), Thrissur - 680 581, **India***
*[5]Institute for Particle Technology (iPAT) and Laboratory for Emerging Nanotechnology (LENA), Technische Universität Braunschweig, Braunschweig 38104, **Germany***

Abstract

A new electrochemical energy storage device, comprising a faradaic rechargeable pseudo-capacitor type electrode with a non-faradaic rechargeable capacitor electrode, is successfully developed for potential applications in smart electric grids. Mapping new electrodes possessing both high energy and power densities as well as long cycle life is vital for the sustainable energy management. In this work, we present a new approach to design electrodes, fabricated from sustainable resources by hybridizing calcined eggshell capacitor anode with a mixed binary metal oxide pseudo-capacitor cathode. Calcium carbonate (calcite), obtained from the biowaste-derived eggshell, is an effective electrode material and operates via accumulation of ions on the electrode surface, providing a high discharge capacitance of 100 F/g through a non-faradaic process. The calcite present in eggshells is found to be a valuable renewable resource which can be utilized for energy storage through suitable process design. Otherwise such potentially useful materials (eggshells) are generally discarded as landfill. The mixed binary metallic oxide (NiO/Co_3O_4) showed a typical pseudocapacitive behaviour associated with both charge transfer reactions and electrostatic means and provided a high discharge capacitance of 225 F/g. The fabricated prototype hybrid device provides an energy density 35 Wh/Kg at a power density 420 W/Kg. The charge storage characteristics of the hybrid device depend heavily on the current rate employed. The design and fabrication of new sustainable electrode materials provides an understanding of materials and their electrochemical performance in the high-voltage window.

***Keywords**: hybrid device; mixed metal oxide; eggshell; cobalt; nickel; calcium; electrochemical*

*minakshi@murdoch.edu.au

Introduction

We are now facing a great challenge to shift from using fossil fuels to renewable energy sources [1]. The demand for renewable and sustainable energy resources has gained a lot of research attention over the past few decades, shaping our views on waste management and climate change mitigation [2]. To make the best use of variable output renewable energy resources, reliable energy storage is important. Among the available energy storage technologies, electrochemical energy storage, including rechargeable batteries and supercapacitors, are currently considered to be the most suitable technology for stationary as well as mobile energy storage applications [3-4]. Energy storage technologies are distinguished by their energy storage mechanisms. Rechargeable batteries store energy through charge transfer reactions, while supercapacitors undergo capacitive charge storage via the formation of an electrochemical double layer (EDL) at the interface between the electrode and the electrolyte [5]. Important characteristics of energy storage devices are the amount of energy that can be stored per unit mass and how fast/quickly the stored energy can be delivered for device performance, while providing required high currents over short durations. This is expressed in energy density (Wh/kg) and power density (W/kg), respectively. Therefore, high-performance energy storage devices that collectively provide high energy density and high power density along with long-term cycling stability are the key features [6]. Unfortunately, typical rechargeable batteries or supercapacitors cannot individually satisfy all of these criteria [7].

To overcome these limitations, several authors have proposed hybridization of a pseudo-capacitor (battery) electrode coupled with a capacitor (EDL) electrode [6-10]. The specific problems associated with either battery or capacitor devices can be offset by proper design and fabrication of a hybrid device [11]. An energy storage system consisting of a battery electrode (cathode) and a capacitor electrode (anode) is called a hybrid device [7] and can meet the demands of both high energy and high power densities suitable for powering smart grids.

So far, extensive research has been carried out and hybrid devices are reported in references [6-17]. Several types of electrodes have been reported [7] and the most commonly used anode materials are biomass-derived carbon for an electrochemical double-layer [18-19]. Likewise, metal oxides and conducting polymers are widely reported as cathode material for such applications [7], which rely on redox-type reactions. It has also been widely accepted in this field that merging carbon material with an electroactive redox (oxide) material leads to a hybrid device with improved performance [7]. In this respect, combinations of activated carbon with MnO_2 in an aqueous electrolyte have gained wide interest [20-21].

Until now, most material designs that have been proposed to enhance the performance characteristics of batteries and supercapacitors have focussed on controlling morphology [22], creating composites with conductive material [23], producing higher surface area [24] etc. But, none of the work on electrodes has focussed on calcium-based technology. In this work, a new approach to energy storage device has been developed, involving the hybridization of a biowaste eggshell anode and mixed metal oxide (NiO/Co_3O_4) cathode in a hybrid system. Mixed binary metal oxides have been investigated as promising electrodes for enhancing supercapacitor properties due to their multiple oxidation states, fast-electron transport access, and high conductivity [25]. However, the synergistic effects of electrochemically deposited mixed metal oxides to allow tuning the properties of the material has not been widely reported for pseudocapacitors. Using biowaste eggshell [26] is not only beneficial for waste management but also creates a value-added product in the market. We have demonstrated the eggshell material in one of our previous reports [26] and have shown its potential to be used in an electrochemical cell. The objective of this work is to fabricate novel electrode materials and to test their electrochemical activity in hybrid devices.

Experimental

Material preparation: The chicken eggshell was obtained from a local supermarket and comprised both calcified shell and shell membranes including inner and outer membranes. These were washed, oven-dried, and then crushed to a powder using a mortar and pestle. The crushed powder was calcined at 600º C for 2 h in air. The Brunauer-Emmett-Teller (BET) surface area of the fine eggshell was 28.22 m^2/g and the cumulative pore size diameter and volume were 9.25 m^2/g and 0.0067 cm^3/g. The mixed metal oxides were deposited from a nitrate aqueous salt solution. The electrodeposition was carried out on a stainless steel (SS) cathode placed in parallel to an Iridium oxide coated Titanium (IrO_2-Ti) anode at a cathodic current density of 200 A m^{-2}. Electro-deposition of mixed Co-Ni oxides were carried out from nitrate solution containing 30 g dm^{-3} $Co(NO_3)_2 \cdot 7H_2O$ + 30 g dm^{-3} $Ni(NO_3)_2$. The final electro-deposited material was a NiO/Co_3O_4 composite. The product was calcined, and yielded a higher surface area of 72.85 m^2/g.

Electrodes for energy storage: For electrochemical measurements, an active electrode was prepared by mixing active material (NiO/Co_3O_4 or calcined eggshell), carbon black and poly-vinylidene fluoride (PVDF) in a 75:15:10 wt.% ratio. All ingredients were mixed in N-methyl-2-pyrrolidone (NMP) solvent to make a slurry which was coated on a small piece of graphite sheet with an active area of 1cm^2.

The electrochemical behaviour of both calcined eggshell and mixed metal oxide materials were investigated with cyclic voltammetry by using a Bio-Logic instrument (SP-150) and galvanostatic charge- discharge techniques by using a Battery Analyser (MTI corporation, USA) operated by a battery testing system (BTS). Electrochemical behaviour of both the electrodes were investigated by using three- electrode cells using 2 M NaOH as an electrolyte. Pt wire and Hg/HgO were used as the counter and reference electrodes, respectively over the

potential range from -0.1─0.6V at various sweep rates. Galvanostatic charge/discharge was carried out in the potential range of 0.2 ─1.6V at various current densities.

For a hybrid device (eggshell vs. NiO/Co_3O_4), to maintain the charge conservation between the two electrodes, the mass ratio was calculated using the below equation (1)

$$m+ /m- = (SC^- * \Delta V^-) / (SC^+ * \Delta V^+) \quad \text{Eq. (1)}$$

where m represents the mass in g. SC^- and SC^+ represents the specific capacitance, ΔV^- and ΔV^+ the discharge/charge potential range for the eggshell and binary metal oxides (i.e. NiO/Co_3O_4), respectively. The specific capacitance and the energy density of the hybrid device were calculated based on the equations reported elsewhere [26]. Based on the single electrode characteristics, shown in one of the results in Fig. 8e, the optimal mass ratio between eggshell and binary metal oxide was determined to be 1.12. Therefore, for a mass of 15 mg binary metal oxide material, the mass of the eggshell was calculated to be 13.4 mg.

Material Characterization: The phase purity of the as-synthesized sample was characterized by powder X-ray diffraction (XRD, Philips PANalytical, Bruker D8) analysis using Mo-Kα radiation at an accelerating voltage and current of 40 kV and 30 mA, respectively. The morphology of the eggshell material was characterized by Mira VP - Field Emission Scanning Electron Microscope (FESEM). High-magnification imaging of the eggshell material was obtained using a scanning transmission electron microscope (STEM) (JEOL ARM200F) operating at 200 kV. STEM specimens were prepared by grinding a small amount of powder in ethanol and dispersing it on a holey carbon film. X-ray photoelectron (XPS) spectra were acquired using a Kratos AXIS Ultra instrument (Kratos Analytical Ltd, U.K.) equipped with a monochromatic Al Kα radiation source (1486.69 eV) operating at 150 W power (15 kV, 10 mA). Analysis chamber pressure was $< 3\times10^{-9}$ mbar. High-resolution spectra acquired for

selected photoemissions were recorded at 0.1 eV/step and with a pass energy of 20 eV. The analysis area was approx. 300 µm x 700 µm.

The particle size of the electrodeposited sample was determined using the LUMiSizer from LUM GmbH. The NiO/Co_3O_4 sample was dispersed in NMP with a concentration of 0.4 wt.% NiO/Co_3O_4 to obtain the first transmission spectra in the range between 30-50%. NMP was used in this experiment as a solvent to emulate the dispersion behaviour of the particles during the slurry preparation of the cathode material. The solution was transferred to a 2 mL polyacrylic cuvette. The particles were made to sediment under three different speeds (300 rpm for 300 s, 2000 rpm for 200 s and 4000 rpm for 200 s). At the end of the measurement, all the particles were sedimented at the bottom of the cuvette. The Ni/Co ratio in the NiO/Co_3O_4 sample was determined using inductively coupled plasma atomic emission spectroscopy ICP-OES (Varian 715-ES) using different wavelengths. For this measurement, the sample was mixed in an aqua regia solution (2 ml HNO_3, double stilled + 6ml HCl (suprapur)) and heated in a closed system at 180 ºC. The solution was then diluted according to the calibration and measured.

Results and Discussion

The crystal structure and purity of the electrodes were examined using X-ray diffraction and the patterns are shown in Fig. 1. The X-ray diffraction pattern of the electrodeposited mixed metal oxide (NiO/Co_3O_4) are in good agreement with the standard patterns for NiO and Co_3O_4 (JCPDS card nos. 47-1049 and 76-1802, respectively). Relatively weak and broader diffraction peaks of NiO suggest a lower crystallinity of the deposited material than the associated Co_3O_4 metal oxide. The Scherrer formula indicates that the average crystallite diameter to be about 30 nm. To retain the amorphous phase and fine grain size, the lower calcination temperature of the nanocomposite oxide is preferred. Calcining the oxide at high temperature ≥ 300 ºC would certainly improve the crystallinity [27], however, it may also affect the surface properties for

the pseudo-capacitor electrode, such as reducing the active surface area. For this reason, it was not carried out here. The X-ray diffraction pattern of the calcined eggshell anode (Fig. 1b) shows narrow diffraction peaks indicating a regular crystalline structure of the calcined eggshell sample. The pattern confirmed that the material was calcite $CaCO_3$ and the peaks are in good agreement with the standard pattern of $CaCO_3$ ((JCPDS card nos. 05-0586). As expected, the primary source of eggshell is calcium in the form of carbonate.

Nanocomposite materials prepared by electrochemical deposition of an active NiO on a supporting Co_3O_4 are of great interest for energy storage applications [28]. To understand the properties of metal oxides, X-ray photoelectron spectroscopy (XPS) surface analysis was carried out on the mixed metal oxides. The XPS survey spectra obtained for the mixed metal oxides is shown in Fig. 2 and high resolution spectra of the elements present are shown in Fig. 3. The surface of the material showed the presence of various elements including Ni and Co and also O and a trace of C. In order to view the spectrum associated with each of the elements presented in Fig. 2, the XPS spectra over regions specific to elements of interest were recorded. Figure 3 shows the high resolution spectra were processed using a Shirley background correction, and were fitted with Gaussian – Lorentzian line shapes. The Ni 2p spectrum (Fig. 3) has significant spin-orbit splitting component of 17.3 eV [28-29]. The multiplet splitting in $Ni2p_{3/2}$ strongly resembles that of NiO [30] and using the same five components as used by Biesinger et al. [31] in their fitting of the Ni 2p spectrum for this compound produced a consistency to the spectrum acquired for the mixed oxide. The O 1s peak confirms this fact exhibiting two components at 529.8 and 531.2 eV due to Ni–O and Ni–OH bonds, respectively. Consequently, it is reasonable to conclude that the Ni in the sample is present as the divalent oxide. The Co 2p spectrum (Fig. 3) has significant spin-orbit splitting component of 14.9 eV with a mixed oxidation state of Co (II) and Co (III). The Co 2p spectrum (Fig. 3) looked like a convolution of the spectrum of Co_3O_4 with that of either $Co(OH)_2$ or CoO or both. The fit

obtained using the components for Co_3O_4 and the hydroxide provided the best fit based on Biesinger et al. [31] in their fitting of spectra for Co, CoO, $Co(OH)_2$, CoOOH, and Co_3O_4. However, the XRD patterns of Co_3O_4 do not show any contributions due to the hydroxides. The N 1s region at 406.7 eV corresponds to nitrate arising from the electrolytic nitrate bath. The C 1s spectrum shows three components: C-C, C-O-C and O-C=O. These are likely due to adventitious carbon contamination. Inductively coupled plasma atomic emission spectroscopy (ICP-AES) was used to determine the elemental ratio of nickel and cobalt in NiO/Co_3O_4. The elemental concentrations are shown in Table 1. The results suggest that the electrode material is composed of 0.72 NiO/0.28 Co_3O_4 and are close to the theoretical ratio, according to the amount added in the electrodeposition process. XPS wide-scan spectrum for calcined eggshell is shown in Fig. 4. Calcium (Ca), Carbon (C), and Oxygen (O) were observed in the samples. Nitrogen (N) was also detected in the calcined sample, at less than 0.2 atom% against 13.7% Ca, and is likely derived from protein in the eggshell membrane. The binding energy value for Ca is in accordance with the reported values for $CaCO_3$ in the literature [32]. The EDS spectrum (Fig. S1) shows the appearance of Ca, O, C without any discernible impurities.

The surface topography of the NiO/Co_3O_4 and calcined eggshell were examined using SEM (Fig. 5). The Ni and Co oxides were intimately mixed at a sub-micron scale and agglomeration of these finer crystals produced clusters with an average diameter of ~ 3 μm. The crystalline structure of the mixed oxides exhibit distinct morphologies of nanopetal like crystallites with a fairly uniform thickness, giving a highly porous texture between the petals, and another area with a sharp contrast of nickel oxides in islands deposited on the Co_3O_4 nanopetals. The corresponding area of the elemental analysis (Fig. S2) confirms the presence of both Ni and Co. The SEM image of calcined eggshell shows it has a much finer scale particle size and poroisty than the mixed oxides. However, for the latter, differentiating between crystal and agglomerate size for the oxides is difficult as this is been electrochemically deposited. To

resolve the ambiguity, particle size distribution of the NiO/Co_3O_4 and calcined eggshell were performed, and the results (Fig. 6). The measured median particle size for NiO/Co_3O_4 and calcined eggshell were 6.55 and 3.24 μm, respectively. The particle size for the oxides agreed with the microscopy result. However, the observed discrepancy for the calcined eggshell suggests the variation in the method of sample preparation. Figures 7 shows the TEM micrographs of both the electrodes; (a-d) calcined eggshell, and (e-h) NiO/Co_3O_4. Fig. 7a shows a bright field TEM imaging of the polycrystalline eggshell clusters and HAADF details thereof are shown Figures 7b-d. These clusters are characterized by being highly porous and nanocrystalline, the crystallites being <50nm in diameter. This type of porosity can play an important role in influencing the adsorption and desorption of ions from the electrolyte [7]. Figure 7e shows the bright field (BF) image of the mixed metal oxides and a detail thereof in Fig. 7f. This shows a range of particle/cluster sizes. EDS mapping (not shown) indicates that all have the same composition. Detailed inspection shows that clusters are comprised of nano-dimensioned nickel oxide particles grown on the cobalt oxide crystallites. The corresponding high-resolution images of the particle shows fine grained (ca 10nm) phase (Fig. 7g) in one area and larger grains (>20nm) in another area (Fig. 7h) indicating the hierarchical arrangement of mixed oxides

The electrochemical behaviour of the mixed metal oxide NiO/Co_3O_4 as cathode and calcined eggshell as anode for a hybrid device were investigated using half-cell performance tests (three-electrode configuration) at various sweep/current rates in the potential range 0 – -1.2 V (for eggshell), and 0 – +0.6 V (for mixed oxides) using Hg/HgO as reference electrode. The anodic performance of the eggshell is shown in Fig. 8a. The cyclic voltammogram (CV) are for various scan rates between 2 and 20 mV s^{-1}. No well-defined peaks (both, during oxidation and reduction) are evident at any sweep rate. This is consistent with the charge-discharge curves observed in the galvanostatic cycling (Fig. 8c). The CV of the eggshell (Fig.

8a) features a quasi-rectangular shape while the charge-discharge processes are almost linear with respect to voltage, and are independent of current. The discharge capacitance 105 F/g. This is similar to what has been observed and reported for various carbon-based electrodes in aqueous electrolytes [18, 33]. The presence of pores in the eggshell facilitates ion transfer in the electrode and ready access of the electrolyte to large areas of electrode, enables the high sweep rates due to capacitance from non-faradaic reaction [34]. The behaviour of NiO/Co_3O_4 (Fig. 8b, d) is quite different with voltage-dependent charge transfer reactions where the potential is a function of initial and final chemical reactions. Well-defined redox peaks (Fig. 8b, C_1 and A_1) were observed for the NiO/Co_3O_4 and these are attributed to the reversible reaction of cobalt and nickel involving the ability of OH^- to be inserted/extracted into/from the NiO/Co_3O_4 electrodes. Individual peaks due to $Co^{2+/3+}$ and $Ni^{2+/3+}$ redox were not resolved in the CV curve because of the fact that the potential for $Co^{2+/3+}$ and $Ni^{2+/3+}$ redox couples are very close. The corresponding charge-discharge curves at different current rates (Fig. 8d) are characteristic of pseudocapacitive oxide electrodes exhibiting an intermediate case (neither purely battery- nor capacitor-type behaviour), and the charge storage corresponds to a capacitance of faradaic nature, termed pseudocapacitance [35]. A typical hybrid device with a working principle is schematically depicted in Fig. 9. The hybrid approach is to combine different type of energy storage materials to achieve high energy and high-power density within a single device. The observed curves (in both Figs. 8b, d) are fundamentally different from the battery electrode, which shows a typical plateau-like discharge/charge curve with a rapid polarization. For this reason, the chosen mixed metal oxide, which exhibits extrinsic pseudocapacitive behaviour, may provide a significant advantage when coupled with an eggshell electrode for a practical device. The nearly symmetric charge-discharge curves imply a high coulombic efficiency and low polarization with a high discharge capacitance of 225 F/g. Translating this capacitance value (F/g) of the mixed metal oxide into capacity (C/g) using the

potential window that is traversed when cycled this device showed an equivalent of 450 C/g. The electrochemical response of this material has been found to be the sum of the responses of the battery- and capacitor-type behaviour involving both faradaic and non-faradaic reactions (as shown in Fig. 9). As shown in Fig. 8d, at a low current density of 0.05 A/g the capacitance contribution is 121 F/g but at a higher current density of 0.2 A/g, the response is dominated by the capacitance showing a contribution of 140 F/g. The mixed metal oxides of Co and Ni are bound to enhance the electronic conductivity which enables the NiO/Co_3O_4 electrode to maintain a relatively high capacitance at higher sweep rates and current densities [36]. The eggshell-derived anode (capacitor) and NiO/Co_3O_4 derived cathode (pseudo-capacitor) shows the performance characteristic (Fig. 8e) of the asymmetric (hybrid) system. The capacitance values for anode and cathode are 105 F/g and 225 F/g, respectively. Based on the mass-balance, a hybrid device comprising two-electrode materials eggshell || NiO/Co_3O_4 was fabricated, with enhanced power and energy characteristics. The CV profile of the device is shown in Fig. 8f. The curves show pseudocapacitive behaviour at lower sweep rate (5 mV/s) based on fast reversible faradaic redox reactions and capacitive behaviour at higher sweep rates (> 5 mV/s) due to fast adsorption and desorption of the electrolyte ions at the interface, respectively [37]. Close inspection of Fig. 8f shows a pair of redox peaks are evident only at the lower sweep rates. It is important to note that the intrinsic properties of the used electrodes, eggshell || NiO/Co_3O_4 are not being altered in the hybrid device, it is the synergy of both electrodes which results in the enhanced energy storage behaviour of binary metal oxide.

The influence of current rates of 0.2 mA and 2 mA on the cell characteristics is shown in Figs. 10 and 11 respectively. Under the same voltage window, the charge-discharge profile at the lower current rate produces a curve with an asymmetric shape (Fig. 10a) while at the higher current rate a symmetric potential profile of shorter duration is seen (Fig. 11a). The asymmetric shape is associated with the redox reactions in the bulk mixed oxide contributing

to the higher capacity. It is noteworthy that the profile in Fig. 10 is suitable for battery applications providing a discharge capacity of 60 mAh/g, whereas, Fig. 11 is suitable for capacitor applications providing a charge capacity of 100 F/g. This is also evident in the respective CV profiles that at a lower scan rate (2 mV/s) prominent redox peaks are seen. These peaks corresponds to an ionic diffusion in the bulk NiO/Co_3O_4 material resulting in reversible faradaic reactions. At a higher scan rate (20 mV/s), the electrochemical energy is contributed by electrostatic force that enhances the electron transfer to the mixed oxide in the hybrid device, leading to better charge transfer reaction at high rates. The synergy between the two electrodes enhanced both the energy density (35 Wh/kg) and power density (420 W/kg) as well as an excellent cycling stability at both low and high charge rates. The calculated capacity retention from the cycling plots for a battery-type (Fig. 10) and supercapacitor-type behaviour (Fig. 11) show that the available capacity is 89.5%, and 95.8%, respectively. The loss in capacity is mainly attributed to the diffusion-controlled response and this is further degraded at higher sweep rates. The delivered stable capacitance of the fabricated hybrid device (95 F/g after 1000 cycles), which is compares favourably with that of similar materials reported for battery-supercapacitor hybrid devices in the literature like Co_3O_4 (57 F/g) [38], $NiCo_2O_4$ (64 F/g) [39], Co – Ni oxides (82 F/g) [40], $CoMoO_4$ (25 F/g) [41] and $NiMoO_4$ (100 F/g) [42] and other ternary metal oxides [43]. Importantly, these reported materials have not used eggshell as anode. The synergistic effect of mixed oxides inhibits the polarization of the electrode suitable for pseudocapacitance, resulting in excellent cycling stability and rate performance.

Conclusions

The hybridization of the electrochemical double layer electrode with a pseudocapacitor electrode enhances the electrochemical properties of the device with a voltage window of 1.6 V. The mixed metal oxide (NiO/Co_3O_4) exhibited a combination of both faradaic reactions at surfaces enabling high capacity (60 mAh/g) and fast charge storage kinetics. The massive OH^-

ion accumulation on the porous oxide electrode resulted in pseudocapacitive reaction. The eggshell showed quasi rectangular CV plots and linear potential-time response in charge-discharge curves with a discharge capacitance of 100 F/g. The islands of NiO grown on the Co_3O_4 nanopetal surface improved the electrical conductivity and shortened the ion diffusion resulting in a psuedocapacitor electrode. The characterization of the electrodeposited sample confirms the presence of Ni and Co in the mixed metal oxide and Ca as the primary resource in the calcined eggshell. ICP-AES analysis showed that synthesis method produced mixed Ni-Co oxides in the expected proportions. The hybrid device delivered a high energy density of 35 Wh/kg and a power density of 420 W/kg with long-term cyclability of 98% retention of initial capacitance. The study clearly indicated that this new hybrid energy storage device, fabricated from bio-waste material like eggshells in combination with available and relatively inexpensive mixed metal oxides (NiO/Co_3O_4) is attractive and has the high potential for many energy intensive applications.

References

1. J. Murray and D. King, Oil's tipping point has passed, *Nature* 481 (2012) 433 – 435.
2. A. Castillo and D. F. Gayme, Grid-scale energy storage applications in renewable energy integration: A survey, *Energy Convers Management* 87 (2014) 885 – 894.
3. B. Zakeri and S. Syri, Electrical energy storage systems: A comparative life cycle cost analysis, *Renewable and Sustainable Energy Reviews* 42 (2015) 569 – 596.
4. B. Dunn, H. Kamath, and J. M. Tarascon, Electrical energy storage for the grid: a battery of choices, *Science* 334 (2011) 928 – 935.
5. H. D. Abruna, Y. Kiya, and J. C. Henderson, Batteries and electrochemical supercapacitors, *Physics Today* 61 (2008) 43 – 47.

6. W. Zuo, R. Li, C. Zhou, Y. Li, J. Xia, and J. Liu, Battery – Supercapacitor hybrid devices: Recent progress and future prospects, *Adv. Sci*. 4 (2017) 1600539.
7. D. P. Dubal, O. Ayyad, V. Ruiz, and P. Gomez-Romero, Hybrid energy storage: the merging of battery and supercapacitor chemistries, *Chem. Soc. Rev*. 44 (2015) 1777 – 1790.
8. F. Wang, X. Wu, X. Yuan, Z. Liu, Y. Zhang, L. Fu, Y. Zhu, Q. Zhou, Y. Wu, and W. Huang, Latest advances in supercapacitors: from new electrode materials to novel device designs, *Chem. Soc. Rev*. 46 (2017) 6816 – 6854.
9. A. Aphale, K. Maisuria, M. K. Mahapatra, A. Santiago, P. Singh, and P. Patra, Hybrid electrodes by in-situ integration of graphene and carbon-nanotubes in polypyrrole for supercapacitors, *Sci. Rep*. 5 (2015) 14445.
10. A. Vlad, N. Singh, J. Rolland, S. Melinte, P. M. Ajayan, and J.-F. Gohy, Hybrid supercapacitor-battery materials for fast electrochemical charge storage, *Sci. Rep*. 4 (2014) 4315.
11. H. S. Choi, J. H. Im, T. H. Kim, J. H. Park, and C. R. Park, Advanced energy storage device: a hybrid BatCap system consisting of battery-supercapacitor hybrid electrodes based on $Li_4Ti_5O_{12}$ – activated-carbon hybrid nanotubes, *J. Mater. Chem*. 22 (2012) 16986 – 16993.
12. D. Zhao, H. Liu, and X. Wu, Bi-interface induced multi-active MCo_2O_4@MCo_2S_4@PPy (M = Ni, Zn) sandwich structure for energy storage and electrocatalysis, *Nano Energy* 57 (2019) 363.
13. H. Liu, D. Zhao, Y. Liu, P. Hu, X. Wu, and H. Xia, Boosting energy storage and electrocatalytic performances by synergizing $CoMoO_4$@$MoZn_{22}$ core-shell structures, *Chem. Engg. Journal* 373 (2019) 485.

14. Y. Zhao, J. He, M. Dai, D. Zhao, X. Wu, and B. Liu, Emerging CoMn-LDH@MnO_2 electrode materials assembled using nanosheets for flexible and foldable energy storage devices*, J. Energy Chem*. 45 (2020) 67.

15. X. Wu, Z. Han, X. Zheng, S. Yao, X. Yang, and T. Zhai, Core-shell structured Co_3O_4@$NiCo_2O4$ electrodes grown on flexible carbon fibres with superior electrochemical properties, *Nano Energy* 31 (2017) 410.

16. D. Zhao, X. Wu, and C. Guo, Hybrid MnO_2@$NiCo_2O_4$ nanosheets for high performance asymmetric supercapacitors, *Inorg. Chem. Frontiers*, 5 (2018) 1378.

17. D. Zhao, M. Dai, H. Liu, L. Xiao, X. Wu, and H. Xia, Constructing High Performance Hybrid Battery and Electrocatalyst by Heterostructured $NiCo_2O_4$@NiWS Nanosheets, *Cryst. Growth Des*. 19 (2019) 1921.

18. Y. Zhang, Z. Gao, N. Song, and X. Li, High-performance supercapacitors and batteries derived from activated banana-peel with porous structures, *Electrochim. Acta* 222 (2016) 1257 – 1266.

19. K. Mensah-Darkwa, C. Zequine, P. K. Kahol, and R. K. Gupta, Supercapcitor energy storage device using biowastes: A sustainable approach to green energy, *Sustainability* 11 (2019) 414.

20. X. Dong, W. Shen, J. Gu, L. Xiong, Y. Zhu, H. Li, and J. Shi, MnO_2 embedded in mesoporous carbon wall structure for use as electrochemical capacitors, *J. Phys. Chem. B* 110 (2006) 6015 – 6019.

21. Z. Cheng, G. Tan, Y. Qiu, B. Gou, F. Cheng, and H. Fan, High performance electrochemical capacitors based on MnO_2/activated carbon paper, *J. Mater. Chem. C* 3 (2015) 6166 – 6171.

22. S. Chen, W. Xing, J. Duan, X. Hu, and S. Z. Qiao, Nanostructured morphology control for efficient supercapacitor electrode, *J. Mater. Chem. A* 1 (2013) 2941 – 2954.

23. N. Zhu, W. Liu, M. Xue, Z. Xie, D. Zhao, M. Zhang, J. Chen, and T. Cao, Graphene as a conductive additive to enhance the high-rate capabilities of electrospun $Li_4Ti_5O_{12}$ for lithium-ion batteries, *Electrochim. Acta* 55 (2010) 5813 – 5818.

24. K. Zhang, B. T. Ang, L. L. Zhang, X. S. Zhao, J. Wu, Pyrolyzed graphene oxide/resorcinol-formaldehyde resin composites as high-performance supercapacitor electrodes, *J. Mater. Chem.* 21 (2011) 2663 – 2670.

25. Y. Zhang, L. Li, H. Su, W. Huang, and X. Dong, Binary metal oxide: advanced energy storage materials in supercapacitors, *J. Mater. Chem. A* 3 (2015) 43 – 59.

26. M. Minakshi, S. Higley, C. Baur, D. R. G. Mitchell, R. T. Jones, and M. Fichtner, Calcined chicken eggshell electrode for battery and supercapacitor applications, *RSC Adv*. 9 (2019) 26981.

27. K. Muller, E. Bugnicourt, M. Latorre, M. Jorda, Y. E. Sanz, J. M. Lagaron, O. Miesbauer, A. Bianchin, S. Hankin, U. Bolz, G. Perez, M. Jesdinzki, M. Lindner, Z. Scheuerer, S. Castello, and M. Schmid, Review on the Processing and Properties of Polymer Nanocomposites and Nanocoatings and Their Applications in the Packaging, Automotive and Solar Energy Fields, *Nanomaterials* 7 (2017) 74.

28. M. M. Natalie, and A. Glisenti, New NiO/Co_3O_4 and Fe_2O_3/Co_3O_4 nanocomposite catalysts: synthesis and characterization, *Chem. Mater*. 15 (2003) 2502 -2510.

29. M. C. Biesinger, B. P. Payne, Leo W. M. Lau, A. Gerson, and Roger St. C. Smart, X-ray photoelectron spectroscopic chemical state quantification of mixed nickel metal oxide and hydroxide systems, *Surface. Interface Analy*. 41 (2009) 324 – 332.

30. A. N. Mansour, Characterization of NiO by XPS, *Surface Science Spectra* 3 (1994) 231.

31. M. C. Biesinger, B. P. Payne, A. P. Grosvenor, Leo W. M. Lau, A. Gerson, and Roger St. C. Smart, Resolving surface chemical states in XPS analysis of first row transition

metals, oxides and hydroxides: Cr, Mn, Fe, Co and Ni, *Appl. Surface Sci.* 257 (2011) 2717 – 2730.

32. M. Ni and B. D. Ratner, Differentiating calcium carbonate polymorphs by surface analysis techniques – an XPS and TOF-SIMS study, *Surface Interface Anal.* 40 (2008) 1356 - 1361.
33. M. Genovese, H. Wu, A. Virya, J. Li, P. Shen, and K. Lian, Ultrathin all-solid-state supercapacitor devices based on chitosan activated carbon electrodes and polymer electrolytes, *Electrochim. Acta* 273 (2018) 392 – 401.
34. Y. Wang, J. Guo, J. Shao, D. Wang, and Y.-W. Yang, Mesoporous Transition Metal Oxides for Supercapacitors, *Nanomaterials* 5 (2015) 1667 – 1689.
35. B. E. Conway, V. Birss, and J. Wojtowicz, The role and utilization of pseudocapacitance for energy storage by supercapacitors, *J. Power Sour.* 66 (1997) 1 – 14.
36. S. Park, S.-K. Kang, and K. Kim, Competition between ionic adsorption and desorption on electrochemical double layer capacitor electrodes in acetonitrile solutions at different currents and temperatures, *J. Power Sour.* 372 (2017) 8 – 15.
37. C. Zhou, H. Du, H. Li, W. Qian, and T. Liu, Electrode based on nanoporous (Co-Ni)@(CoO,NiO) nanocomposites with ultrahigh capacitance after activation*, J. Alloys and Compds.* 778 (2019) 239 – 246.
38. W. Liu, X. Li, M. Zhu, and X. He, High-performance all-solid state asymmetric supercapacitor based on Co_3O_4 nanowires and carbon aerogel, *J. Power Sour*. 282 (2015) 179 -186.
39. J. Zhu, J. Jiang, Z. Sun, J. Luo, Z. Fan, X. Huang, H. Zhang, and T. Yu, 3D Carbon/Cobalt-Nickel Mixed-Oxide Hybrid Nanostructured Arrays for Asymmetric Supercapacitors, *Small* 10 (2014) 2937-2945.

40. J. Zhang, F. Liu, J. P. Cheng, and X. B. Zhang, Binary Nickel-cobalt Oxides Electrode Materials for High-performance Supercapacitors: Influence of its Composition and Porous Nature, *ACS Appl Mat. Interfaces*, 7 (2015) 17630–17640.
41. M. J. Barmi and M. Minakshi, Role of polymeric surfactant in the synthesis of cobalt molybdate nanospheres for hybrid capacitor applications. *RSC Adv*. 6 (2016) 36152-36162.
42. T. Chen, R. Shi, Y. Zhang, and Z. Wang, A $MnCo_2O_4$@$NiMoO_4$ Core-Shell Composite Supported on Nickel Foam as a Supercapacitor Electrode for Energy Storage, *ChemPlusChem* 84 (2019) 69 – 77.
43. Y.-Y. Huang, and L.-Y. Lin, Synthesis of ternary metal oxides for battery-supercapacitor devices: influences of metal species on redox reaction and electrical conductivity, *Adv. Energy Mater*. 1 (2018) 2979 – 2990.

Table 1 ICP-AES analysis of NiO/Co_3O_4 material

Electrode	Concentration of Ni (ppm)	Concentration of Co (ppm)	Molar ratio of Ni/Co
NiO/Co_3O_4	3.40×10^5	4.22×10^5	1:1.24

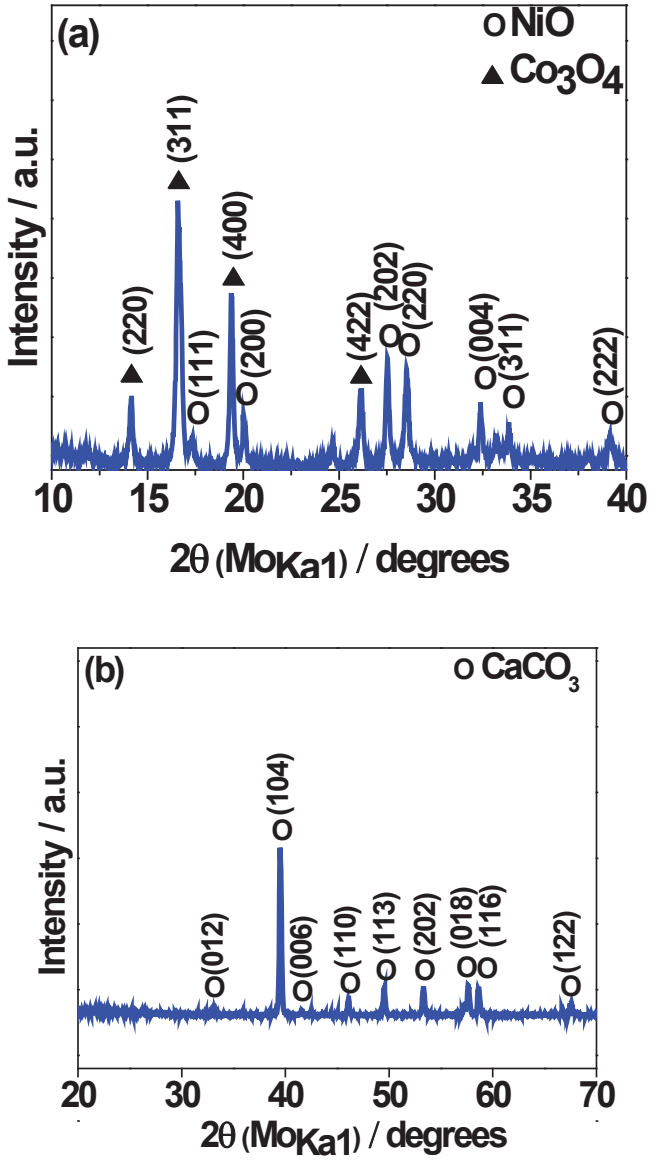

Figure 1 X-ray diffraction patterns of: a) mixed metal oxides electrodeposited from a nitrate bath resulting in a mixed transition metal oxide (NiO/Co_3O_4) ; b) calcined eggshell powder resulting in $CaCO_3$.

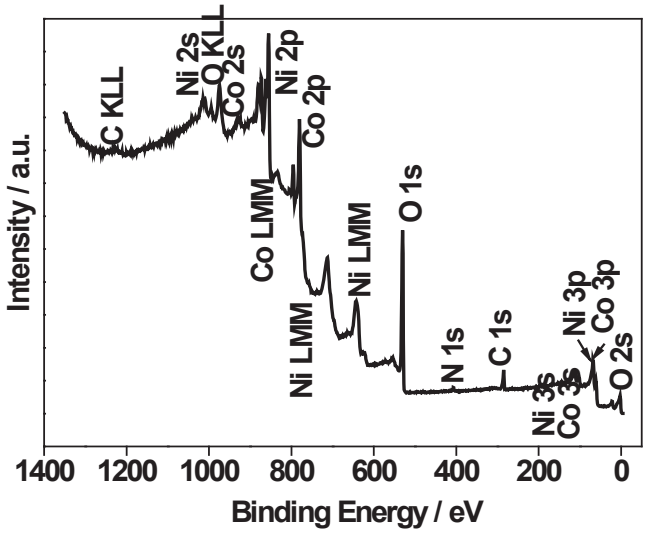

Figure 2 Wide scan XPS spectra of electrodeposited mixed transition metal oxide (NiO/Co_3O_4) powder showing the elements present.

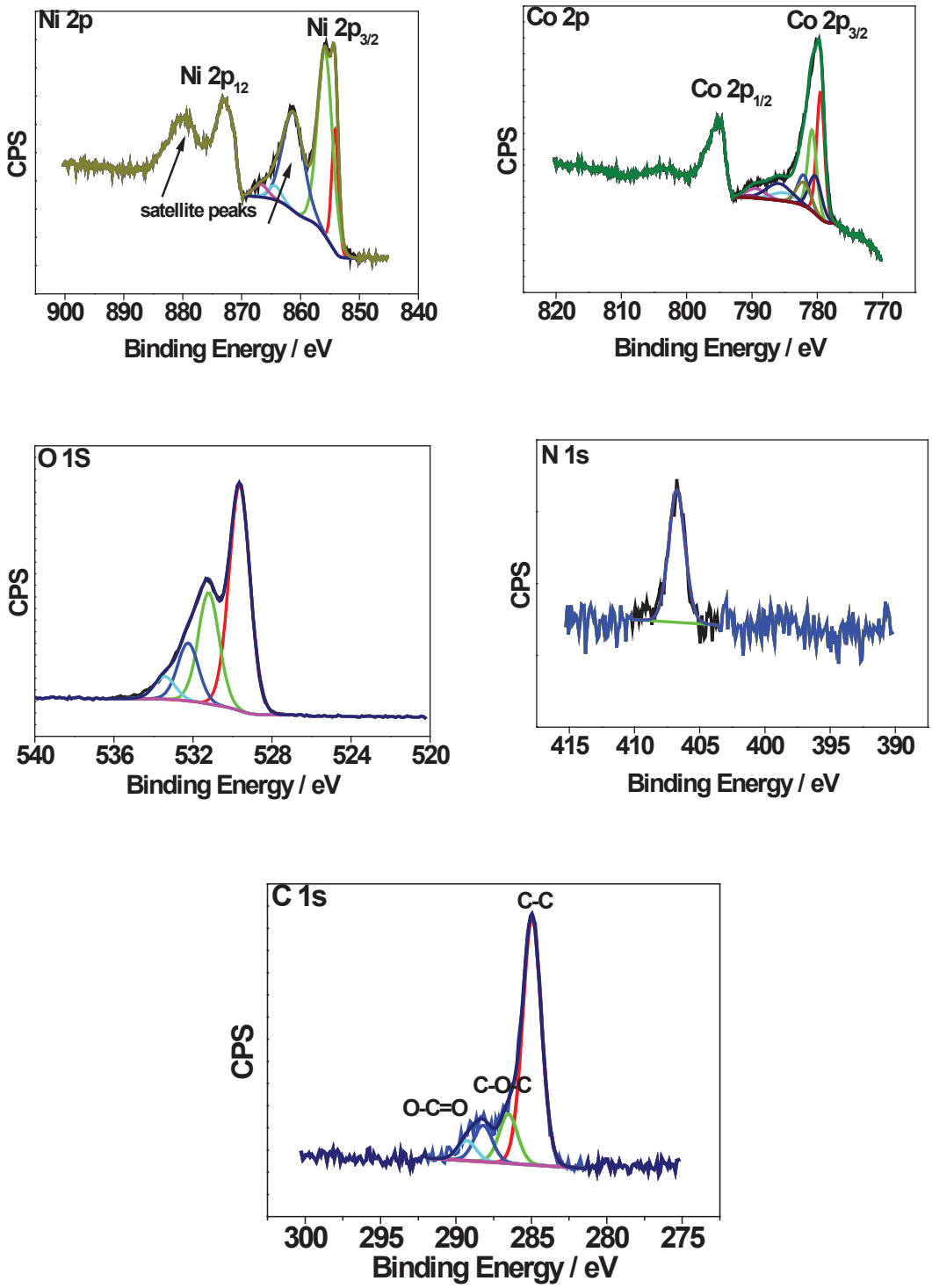

Figure 3 High-resolution XPS spectra of electrodeposited mixed transition metal oxide (NiO/Co_3O_4) powder showing spectral regions for : a) Ni 2p; b) Co 2p; c) O 1s; d) N 1s and e) C 1s.

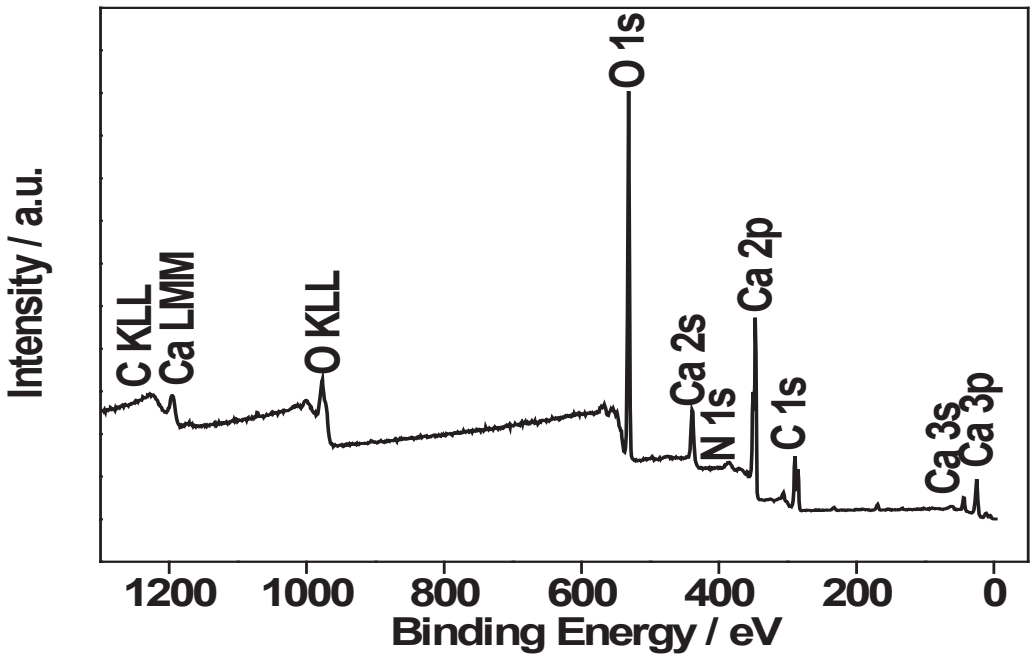

Figure 4 Wide scan XPS spectra of calcined chicken eggshell powder showing the elements present in the shell.

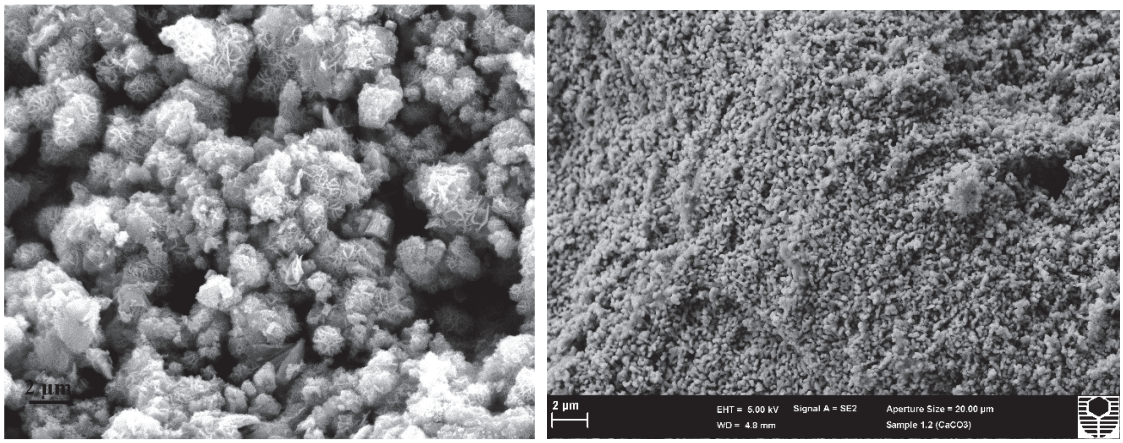

Figure 5 SEM secondary electron images of the electrodeposited mixed transition metal oxide (NiO/Co_3O_4) (left), and calcined chicken eggshell (right) under the same magnification.

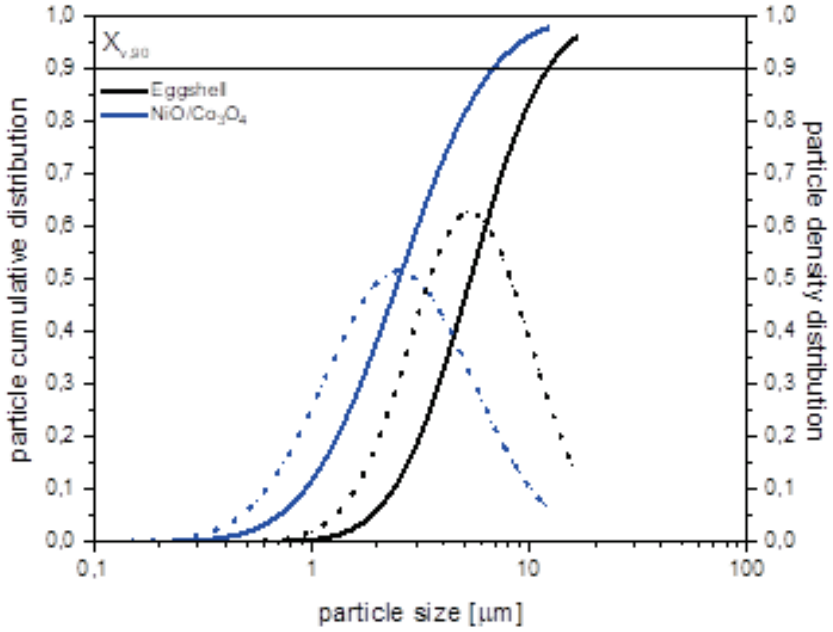

Figure 6 Particle cumulative (solid line) and density (dotted line) distribution of $CaCO_3$ and NiO/Co_3O_4

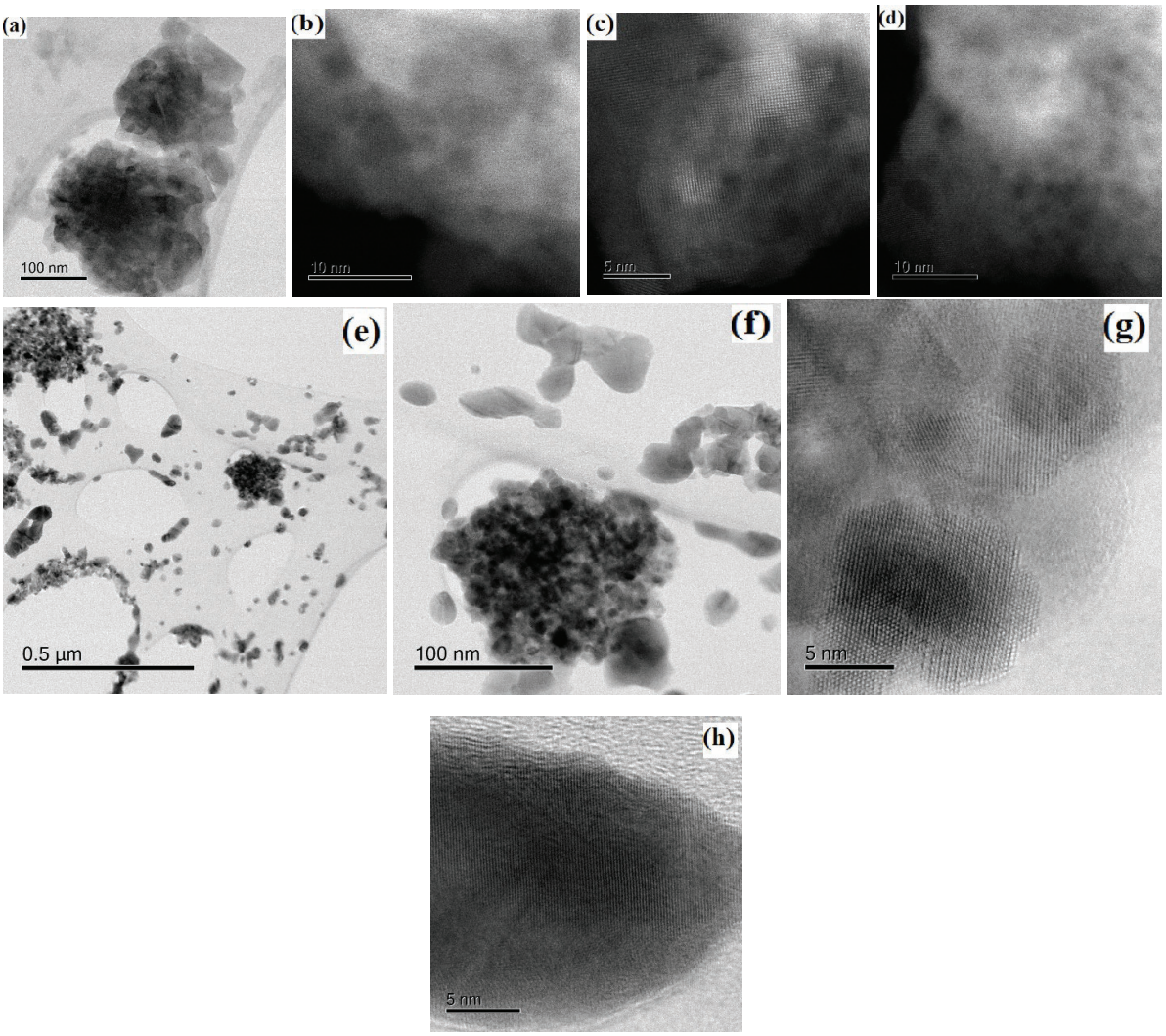

Figure 7 STEM bright field images of (a-d) calcined eggshell, and (e-h) NiO/Co_3O_4 mixed oxides.

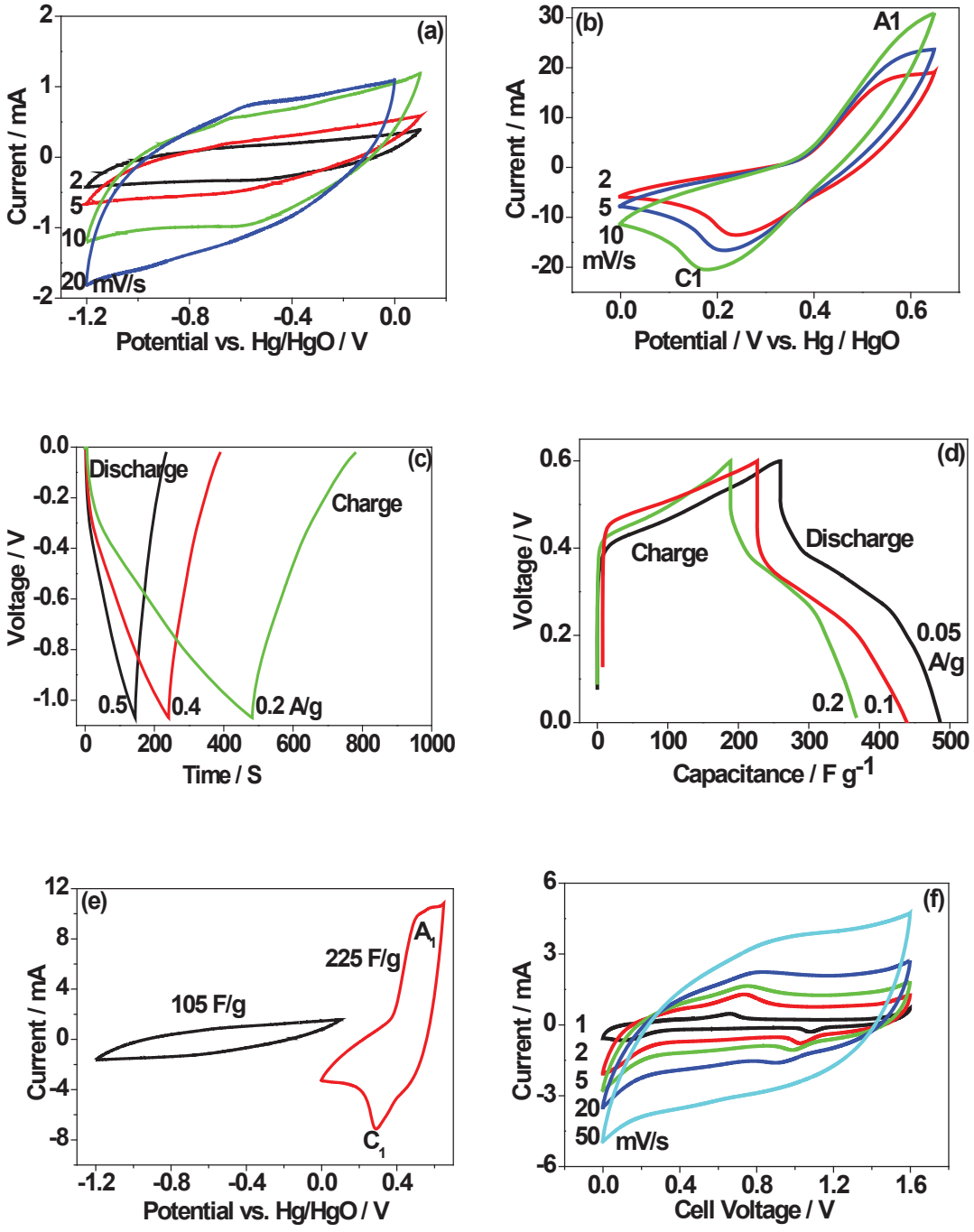

Figure 8 First cyclic voltammetric (CV) curves of (a) calcined eggshell, and (b) mixed metal oxides electrode at different scan rates shown in the respective figures. Charge-discharge behaviour (three-electrode configuration) of (c) eggshell in the negative region, and (d) mixed metal oxides in the positive region at different current rates shown. (e) CV curves of eggshell as negative (black curve) compared with mixed metal oxides (red curve) as positive electrode. CV curves of hybrid cell (two-electrode configuration) (f) comprising a supercapacitor eggshell || NiO/Co_3O_4 in 2M NaOH aqueous electrolyte. Curves show pseudocapacitive behaviour at lower sweep rates (< 5 mV/s), and capacitive behaviour at higher sweep rates (> 5 mV/s), respectively.

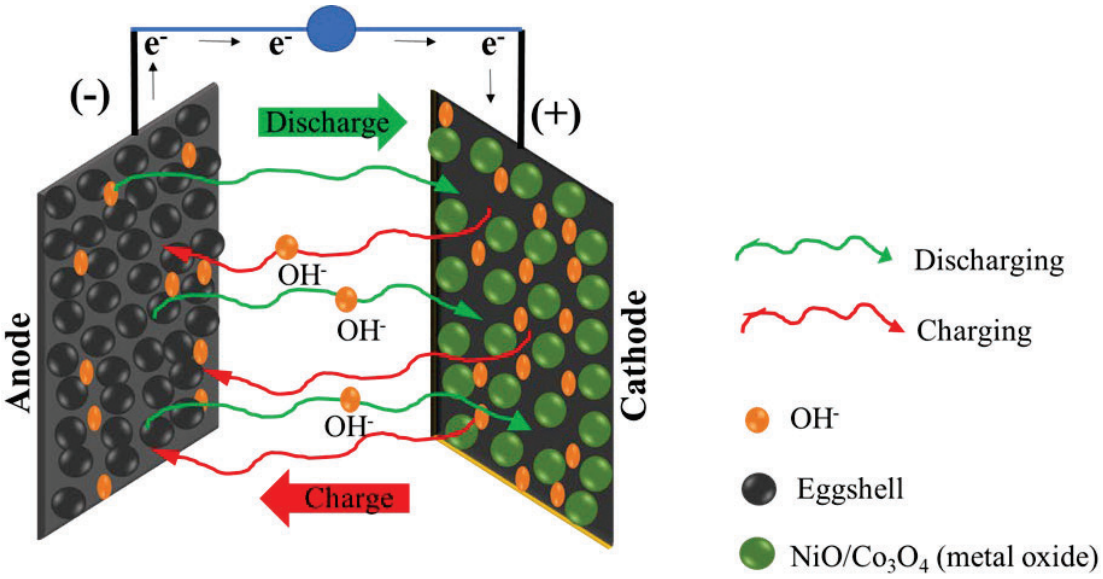

Figure 9 Schematic of a hybrid device (eggshell || NiO/Co_3O_4) showing the working principle during an electrochemical (charge/discharge) processes.

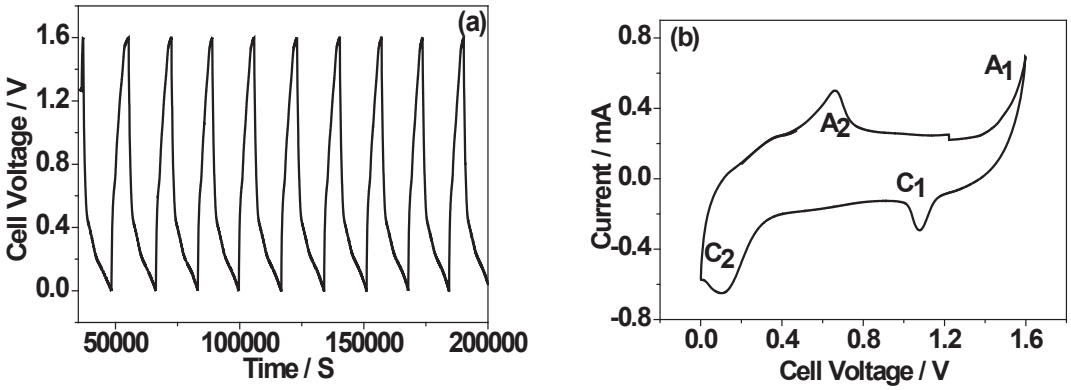

Figure 10 Hybrid cell (two-electrode configuration) (a) CV and (b) charge-discharge curves for consecutive cycles of supercapacitor comprising eggshell || mixed metal oxides at a lower current rate of 0.2 mA. Both CV and charge-discharge curves show well-defined redox peaks implying a battery-like behaviour at this current.

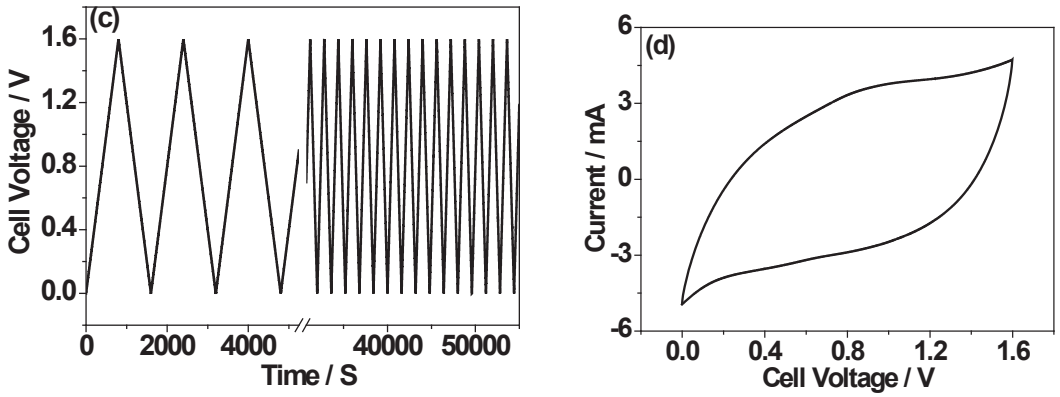

Figure 11 Hybrid cell (two-electrode configuration) (a) CV and (b) charge-discharge curves for consecutive cycles of supercapacitor comprising eggshell || mixed metal oxides at a higher current rate of 2 mA. Both CV and charge-discharge curves show quasi-rectangular like redox curves implying capacitive behaviour of 2 mA.

Supporting Information (SI)

This supporting information (SI) contains two figures.

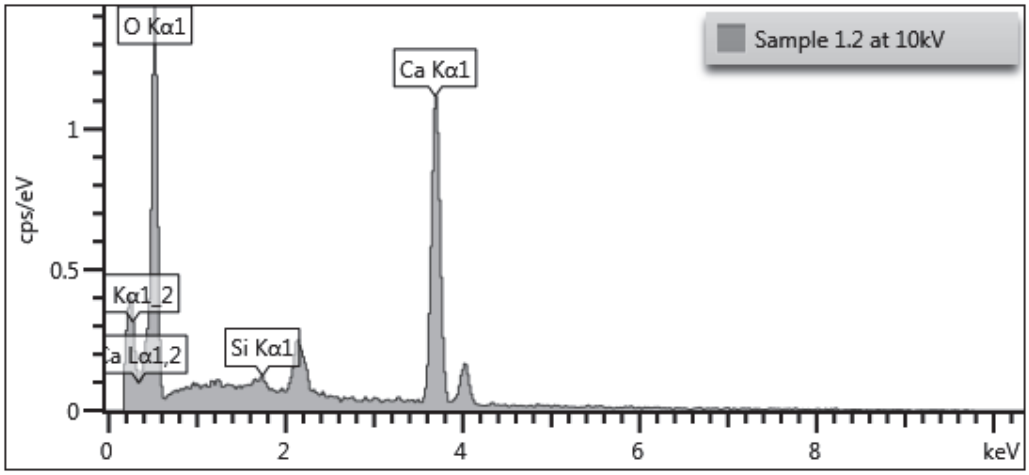

Figure S1 EDS spectrum of the calcined eggshell ($CaCO_3$) showing the elements present in it.

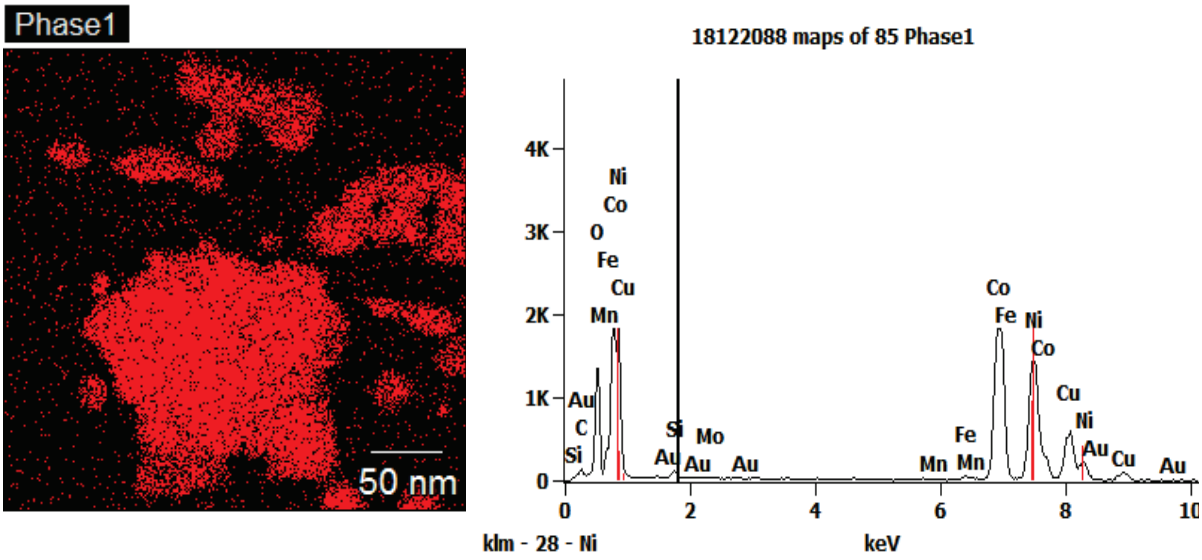

Figure S2 Elemental mapping (left) and the corresponding EDS spectrum (right) of the mixed metal oxide NiO/Co_3O_4 showing a uniform Co and Ni distribution, even in particles as small as 10nm.